APS AWARD PAPERS

The paper in this section is based on the 2001 Otto LaPorte Award Lecture, presented at the 54th Annual Meeting of the American Physical Society's Division of Fluid Dynamics, San Diego, CA, 16–18 November 2001.

Control of turbulent boundary layers

John Kim
Department of Mechanical and Aerospace Engineering, University of California, Los Angeles, California 90095-1597

(Received 9 September 2002; accepted 15 January 2003; published 21 March 2003)

The objective of this paper is to give an overview of recent progress on boundary layer control made by the author's research group at University of California, Los Angeles. A primary theme is to highlight the importance of a certain linear mechanism and its contribution to skin-friction drag in turbulent boundary layers—and the implication that significant drag reduction can be achieved by altering this linear mechanism. Examples that first led to this realization are presented, followed by applications of linear optimal control theory to boundary-layer control. Results from these applications, in which the linear mechanism in turbulent channel flow was targeted, indirectly confirm the importance of linear mechanisms in turbulent—and hence, nonlinear—flows. Although this new approach has thus far been based solely on numerical experiments which are yet to be verified in the laboratory, they show great promise and represent a fundamentally new approach for flow control. The success and limitations of various controllers and their implications are also discussed. © *2003 American Institute of Physics.* [DOI: 10.1063/1.1564095]

I. INTRODUCTION

Control of turbulent flows, turbulent boundary layers in particular, has been a subject of much interest owing to the high potential benefits. Skin-friction drag, for example, constitutes a large fraction of the total drag on commercial aircrafts and cargo ships, and any reduction entails substantial savings of the operational cost for commercial airlines and cargo-shipping industries.[1] Enhanced mixing in combustion engines, enhanced heat transfer in heat exchangers, or reduced heat transfer to gas-turbine blades are only a few examples that also illustrate the immediate benefits of turbulence control. Successful control, however, requires both a thorough understanding of the underlying physics of turbulent flow and an efficient control algorithm, the current state of which leaves much room for improvement.

Significant progress has been made recently by combining computational fluid dynamics, control theories, and sensor/actuator technologies. Direct numerical simulation (DNS) and large-eddy simulation (LES), despite being limited to relatively simple and moderate Reynolds-number flows, have provided much needed detailed information, from which insight into turbulent flow physics can be gained. Our understanding of the physics of turbulent boundary layers and free-shear flows has been significantly improved in large part due to DNS and LES of these flows over the past two decades.[2]

Most early attempts of turbulence control were based on the investigator's intuition and/or on a trial-and-error basis. Several investigators have recently started applying more systematic approaches to controller design. These approaches are significantly different from previous ones in that modern control theories are incorporated into the controller design. Some of these new approaches and their relationships to each other will be discussed below.

Properly designed controllers require appropriate sensors and actuators. This has been a critical issue for turbulence control, boundary-layer control in particular, because the time and length scales associated with the turbulent eddies to be controlled are extremely small at the Reynolds numbers of engineering applications, thus requiring a large number of small sensors and actuators with high-frequency response. Micro-electro-mechanical systems (MEMS) technology will play an essential role in producing arrays of a large number of sensors and actuators at a reasonable cost. The possibility of utilizing MEMS technology in producing such sensors and actuators has been demonstrated recently by the UCLA–Caltech group. They were able to fabricate sensors, actuators, and simple control logic onto a chip, thus illustrating, at least in principle, that MEMS technology can produce the large number of sensors and actuators necessary for turbulence control. Interested readers are referred to Tsao *et al.*[3] and Ho and Tai,[4] for applications of MEMS technology to boundary layer control and general fluid dynamics, respectively.

The objective of this paper is to provide an overview of recent progress made by the author's research group at University of California, Los Angeles (UCLA). Particular emphasis is upon nontraditional approaches using modern control theory (see, for example, Zhou *et al.*[5]). Other research groups [University of California, San Diego (UCSD), University of California, Santa Barbara (UCSB), Stanford in the

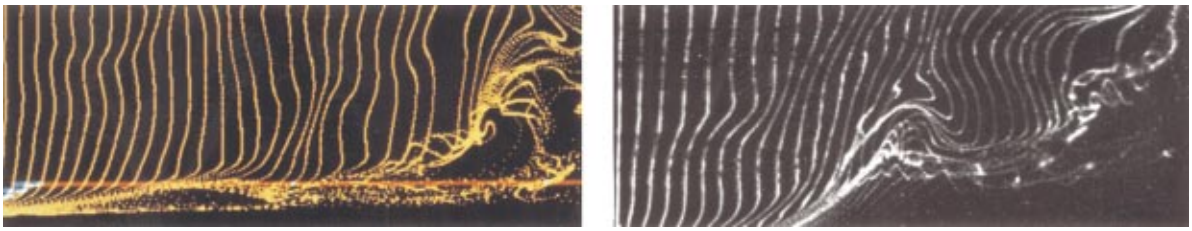

FIG. 1. (Color) Marker particles in a motion picture of a simulated flow (left) and hydrogen bubbles in a laboratory experiment by Kline *et al.* (Ref. 9) (right).

US, and Kungal Tekniska Högskolan (KTH) in Sweden, to name a few] are conducting similar research, but they are not discussed here as they were outside the scope of the lecture upon which this paper is based. I mention in passing that the work carried out by researchers at UCSD, UCSB and KTH is very closely related to that described in Sec. IV D, while that by the Stanford group is similar to those described in Secs. IV A and IV C.

This paper is organized as follows. A brief account of the history of an early numerical simulation of turbulent channel flow, which is viewed by many as a starting point for establishing numerical simulation of turbulent flows as a viable tool for turbulence research, is given in Sec. II. In Sec. III a brief discussion of the skin-friction drag in turbulent boundary layers is given. Various approaches aimed at reducing the skin-friction drag, especially from the perspective of controlling a key linear mechanism, are presented in Sec. IV. Issues and limitations associated with turbulence control, and a concluding remark, are given in Sec. V.

In this paper, I shall use (x,y,z) for the streamwise, wall-normal, and spanwise directions, respectively, and (u,v,w) for the corresponding velocity components unless stated otherwise. The superscript $+$ denotes flow quantities nondimensionalized by the wall-shear velocity, u_τ, and the kinematic viscosity, ν.

II. ILLIAC IV AND TURBULENT CHANNEL SIMULATIONS

The direct numerical simulation of turbulent channel flow presented in this paper as examples of various control experiments has its origin in the late 1970s, when I began working at NASA Ames Research Center. The original computations[6] were carried out on a very unique computer called ILLIAC IV, which had just been brought into NASA Ames Research Center from the University of Illinois.[7] The ILLIAC IV was, to the best of my knowledge, the first large-scale parallel computer with 64 processors (called processing elements or PEs). Although it was huge and required an entire building to house it, the computer had very limited power by present-day standards. For example, it had the total of only one megabyte of memory (each PE had 2048 64-bit words of memory). Asynchronous data transfer between the core memory and external memory, which consisted of 13 4-foot diameter disks, each with 9.8 megabytes of memory (128 megabytes in total), was designed and used for ''large-scale'' computations. Homemade compilers were written by Ames scientists Bob Rogallo (CFD) and Alan Wray (Vectoral) to replace the compiler supplied with the machine, since it was so unreliable. The ILLIAC IV typically ran with

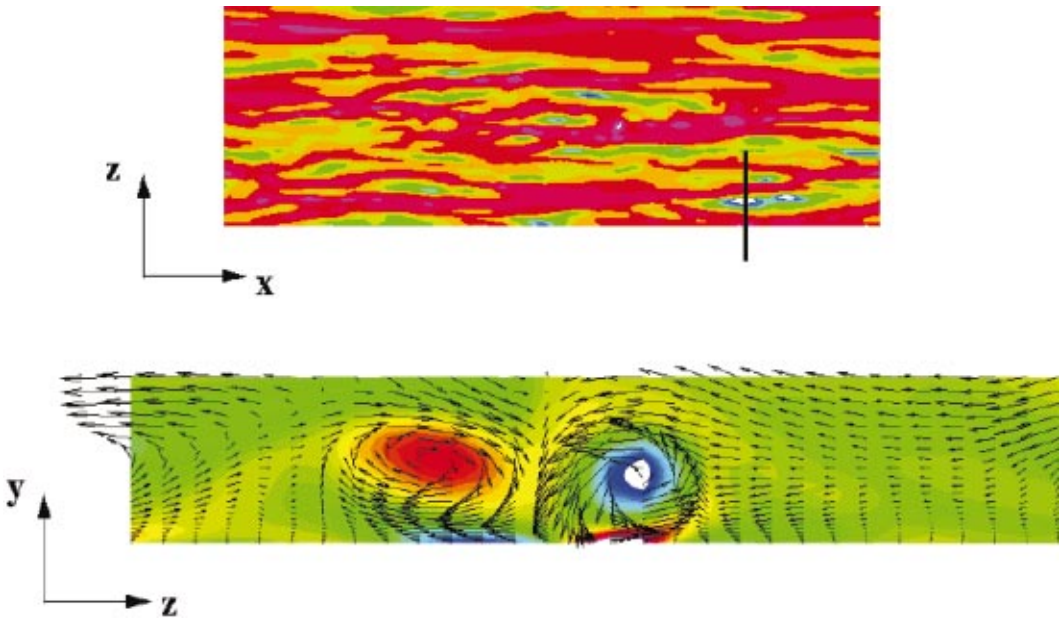

FIG. 2. (Color) Skin-friction in turbulent boundary layers. Plan view of contours of spanwise vorticity at the wall, showing high skin-friction regions indicated by blue and green (top). Cross section view of the high skin-friction region marked by the straight line in the top figure (lower right corner), showing a pair of streamwise vortices in the wall region. Colors denote the magnitude of streamwise vorticity while the vectors indicate the wall-normal and spanwise components of the velocity in the plane (bottom).

the clock at 12.5 MHz, and an optimized code like our plane-channel solver could achieve about 20 Mflops in 64-bit mode and 30 Mflops in 32-bit mode.[8]

With this then-powerful and unique computer, we performed the large-eddy simulation (LES) of turbulent channel flow.[6] At first, it was not very well received, especially by experimentalists, despite the fact that computed turbulence statistics were in good agreement with measured ones. In order to convince the skeptics, and perhaps to some extent ourselves, we produced computer-generated motion-picture visualizations from the simulated flow field, which closely mimicked laboratory visualizations using hydrogen-bubble wires in water[9] (see Fig. 1). This visualization, now common in computational fluid dynamics, was unusual at the time, and was instrumental in convincing many experimentalists who had previously been skeptical of the validity of numerical simulations. This computer-generated movie thus helped establish large-scale computations as an equal partner with laboratory experiments as a turbulence research tool.

III. SKIN-FRICTION DRAG IN TURBULENT BOUNDARY LAYERS

Although it has been common knowledge in fluid mechanics that the skin-friction drag in turbulent boundary layers is much higher than that in laminar boundary layers, it was not until recently that we began to understand why this was the case. Since the underlying physics of high skin-friction drag were not known, most attempts to reduce the drag were on a trial-and-error basis.

Existence of well-organized turbulence structures and the recognition that these structures play important roles in the wall-layer dynamics are among the major advances in turbulent boundary layer research during the past several decades. The ubiquitous structural features in this region are low- and high-speed ''streaks,'' which consist mostly of a spanwise modulation of the streamwise velocity. These streaks are created by streamwise vortices, which are roughly aligned in the streamwise direction. It has now been recognized, in large part due to numerical investigations, that streamwise vortices are also responsible for the high skin-friction drag.[10,11] These vortices are primarily found in the buffer layer ($y^+=10-50$) with their typical diameter in the order of $d^+=20-50$.[12] There is strong evidence that most high skin-friction regions in turbulent boundary layers are induced by nearby streamwise vortices (Fig. 2). These vortices are formed and maintained autonomously (independent of the outer layer) by a self-sustaining process, which involves the wall-layer streaks and an instability associated with them.[13–16]

In light of this description, we asked the following question for the purpose of boundary-control for drag reduction: ''Can we suppress (or mitigate) the formation of these streamwise vortices through an actuation at the wall, and if so, would it lead to a significant reduction of the skin-friction drag?'' The remainder of this paper addresses this question by reviewing various approaches that have been used in an attempt, directly or indirectly, to reduce the impact of streamwise vortices on the skin-friction drag in turbulent boundary layers. In particular, we examine a linear mechanism associated with these streamwise vortices, and present controllers designed to suppress the linear mechanism. The success of these controllers demonstrates that this linear mechanism plays an important role, although the boundary layer on the whole is governed by nonlinear dynamics.

This paper discusses active feedback control, which involves actuation and sensing, nominally at the wall. We mention here in passing that passive control, which requires no actuation (i.e., no external energy input), has also been tried. One successful example, which has been shown to reduce the skin-friction drag (a maximum on the order of 5–7 %), involves riblets. These are surfaces with narrow grooves aligned in the streamwise direction. It is noteworthy that the riblet surface also reduces the skin-friction drag by interfering with the interactions between the streamwise vortices and the wall.[10] The interested reader is referred to Choi *et al.* and the references therein.

IV. NUMERICAL EXPERIMENTS

All examples presented in this paper, unless stated otherwise, have been obtained in a turbulent channel with unsteady blowing and suction at the wall as control input, which was determined by various feedback control laws. Details of the numerical methods[17] can be found in Kim *et al.*[12] All numerical experiments have been performed at very low Reynolds numbers, $\mathrm{Re}_\tau=100-200$, where Re_τ denotes the Reynolds number based on the wall-shear velocity and channel half-width. Implications related to the low Reynolds number flows are addressed in Sec. V.

A. Opposition control

In an attempt to mitigate the effect of streamwise vortices in the buffer layer, Choi *et al.*[18] used blowing and suction at the wall equal and opposite to the wall-normal component of velocity at $y^+=10$ (Fig. 3). They showed that this simple control, now known as *opposition control*,[19] resulted in approximately 25–30 % drag reduction in a turbulent channel flow. The computed flow fields were examined to determine the mechanism by which the drag reduction was achieved. The most salient feature of the controlled flow field was that the strength of the near-wall streamwise vortices was substantially reduced, and consequently most of the high skin-friction regions were suppressed, resulting in the mean drag reduction.

Although the method employed in opposition control is impractical, as the information at $y^+=10$ is normally not

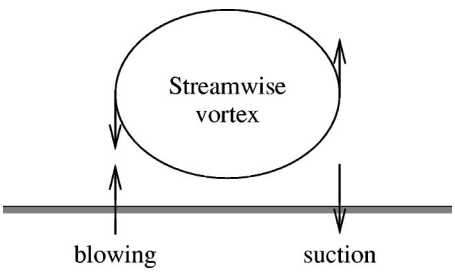

FIG. 3. A schematic illustrating opposition control.

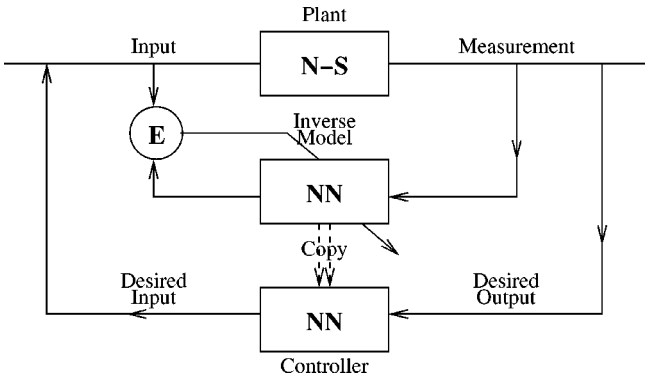

FIG. 4. A schematic illustrating a neural network representing an adaptive inverse model of the Navier–Stokes plant.

available, it conveys a significant message for our purpose: it demonstrates that manipulation of the near-wall streamwise vortices does indeed lead to substantial reduction of the skin-friction drag in turbulent boundary layers. Opposition control has been used as a reference case to which other control schemes can be compared.

B. Adaptive inverse model

In order to circumvent the problem associated with opposition control, Lee *et al.*[20] used wall actuation, which depends only on flow quantities that can be measured at the wall. They designed and trained a neural network, which served as an adaptive inverse model of the plant represented by the Navier–Stokes equations (Fig. 4). The network was trained to predict actuation at the wall (control input) for given outputs at the wall. Once properly trained, this inverse model network was used as a controller to predict an optimal control input for a desired output, i.e., reduced skin-friction drag. A schematic illustrating a neural network representing an adaptive inverse model of the Navier–Stokes equations is shown in Fig. 4.

Details of their neural network are given in Lee *et al.*[20] The functional form of the final neural network is

$$v_{jk} = W_a \tanh\left(\sum_{i=-(N-1)/2}^{(N-1)/2} W_i \left.\frac{\partial w}{\partial y}\right|_{j,k+i} - W_b \right) - W_c ,$$

$$1 \leqslant j \leqslant N_x \quad \text{and} \quad 1 \leqslant k \leqslant N_z , \tag{1}$$

where W denotes weight, N is the total number of input weights, and the subscripts j and k denote the numerical grid point at the wall in, respectively, the streamwise and spanwise directions. N_x and N_z are the number of computational grid points in each direction. The summation is done over the spanwise direction. Seven neighboring points ($N=7$), including the point of interest, in the spanwise direction (corresponding to approximately 90 wall units) were found to provide enough information to adequately train and control the near-wall structures responsible for the high skin friction. Note that the input to the neural network is $\partial w/\partial y$ at the wall, not $\partial u/\partial y$. Initially $\partial u/\partial y$ and $\partial w/\partial y$ at the wall at several instances of time were used as input data fields, and the actuation at the wall was used for the output data of the network. Experimentally we found that only $\partial w/\partial y$ at the wall from the current time was necessary for successful network performance.

Applying this control scheme to a turbulent channel flow at low Reynolds numbers resulted in about 20% drag reduction. The computed flow fields were examined and it was found that instantaneous flow patterns were very similar to those observed in the opposition-controlled channel, i.e., the strength of the near-wall streamwise vortices was substantially reduced (Figs. 5 and 6). This result further substantiates the notion that successful suppression of streamwise vortices leads to a significant reduction in the skin-friction drag. It is worth mentioning here, however, that there may be other flow quantities that have a more direct link to the reduced skin-friction drag, but these we have not yet explored.

An examination of the weight distribution from the online neural network led to a very simple control scheme that worked equally well while being computationally more efficient. This simple control scheme indicated that the optimum blowing and suction at the wall should be in the form

$$v_w \sim \overline{\left.\frac{\partial}{\partial z}\frac{\partial w}{\partial y}\right|_w} , \tag{2}$$

where the overbar represents a local spatial average with high wavenumber components properly reduced (see Lee *et al.*[20] for details). The converged weight distribution can be expressed analytically, thus making the implementation of this control scheme relatively easy.

The simple pattern of the weight distribution derived from the nonlinear network suggests the possibility of using a linear network. A linear neural network, identical to that of Eq. (1) without the hyperbolic tangent function, was applied to the same problem. This linear network resulted in almost identical drag reduction with instantaneous flow patterns very similar to those obtained by the original nonlinear network. The success of this linear network suggests that the flow dynamics of interest, i.e., those relevant to high-skin friction, can be approximated by a linear model, the implication of which will be further explored in the remainder of this paper.

C. Adjoint-based supoptimal control

As mentioned in the Introduction, most previous control work has been rather *ad hoc*, in that it was primarily based on the investigator's intuition and insight into the flow physics under consideration. The *opposition control* is a good example. More systematic approaches, relying on the equations that govern the problem under control, have appeared recently. One such approach is adjoint-based optimization.[21–24] In this approach the control objective is to minimize a cost functional, $J(\phi)$, of control input, ϕ. Once the sensitivity of the cost functional with respect to the control input is known, it can be minimized by using any gradient-based iteration scheme. For example,

$$J(\phi^{k+1}) = J(\phi^k) + \frac{DJ}{D\phi}(\phi^{k+1} - \phi^k), \tag{3}$$

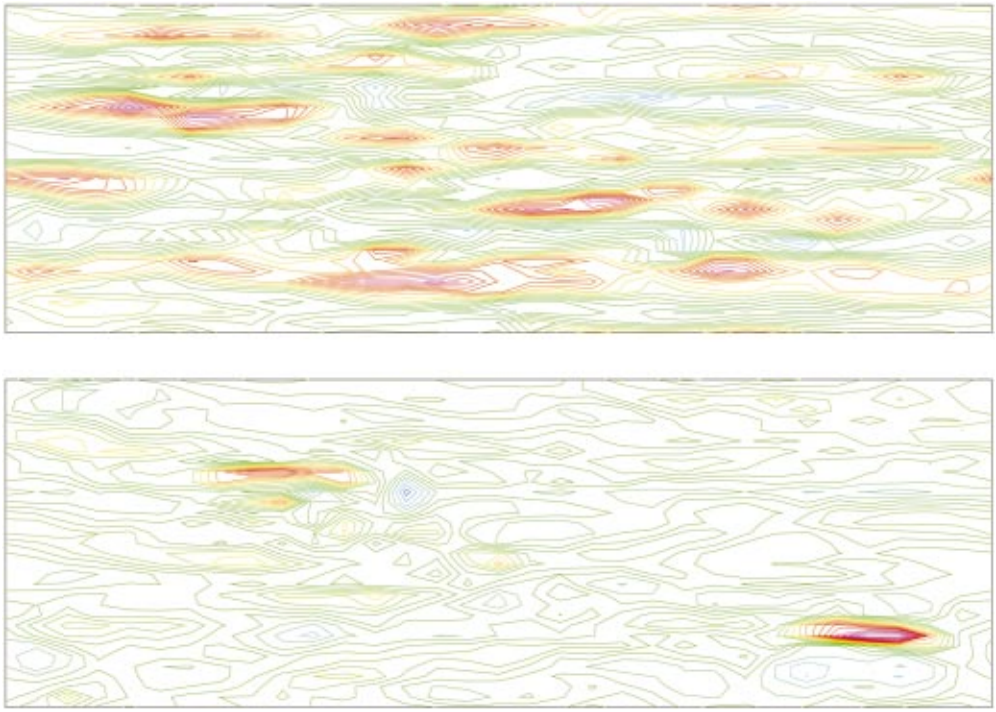

FIG. 5. (Color) Contours of streamwise wall-shear stress in (x,z)-plane in regular (top) and NN-controlled (bottom) channel.

where $DJ/D\phi$ is the Fréchet differential of J, representing the sensitivity of the cost functional to the control input. More advanced iterative schemes, such as a conjugate-gradient method, could also be used, instead of the simple gradient method shown here. A key step is how to evaluate the sensitivity functional. A popular approach has been to express it in terms of properly defined adjoint flow variables, which can be obtained by solving adjoint governing equations. In general, one has to solve the Navier–Stokes equations and the adjoint Navier–Stokes equations simultaneously. Interested readers are referred to the references given above for further details.

Bewley *et al.*[24] applied an adjoint-based optimal control, in which a control objective was minimized over a finite time

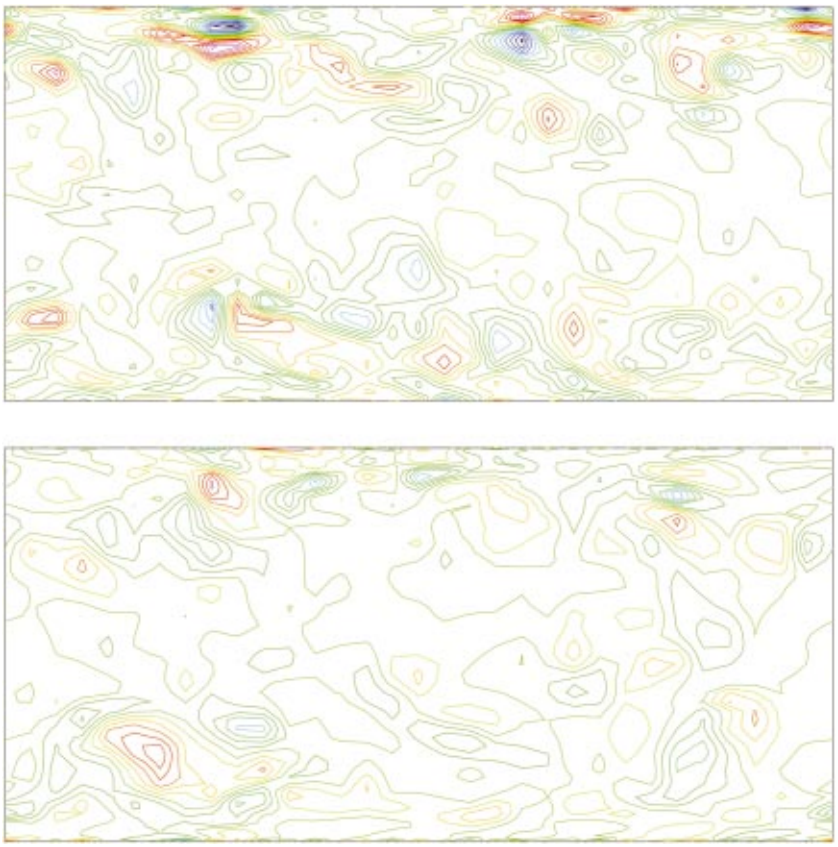

FIG. 6. (Color) Contours of streamwise vorticity in (y,z)-plane in regular channel (top) and NN-controlled channel (bottom).

period, to a turbulent channel at $\mathrm{Re}_\tau = 100$. Their approach led to flow laminarization with a drag reduction of over 50%. However, this algorithm requires solving the Navier–Stokes equations and their adjoint equations iteratively over a finite time period (referred to as finite-time horizon); while the adjoint equations are integrated backward in time, the Navier–Stokes equations are integrated forward in time, during which the control input, which in turn depends on the adjoint variables, is required. This procedure is computationally expensive, and more importantly, impossible to implement in practice. Nevertheless, this is an important accomplishment on several accounts. For example, it demonstrates that a control algorithm derived rigorously from a control theory independent of flow physics can outperform intuition-based controls. Also, notwithstanding its practical limitation, it establishes the best possible control process, from which physical insight may be gained by examining the manner in which the laminarization occurred. The adjoint-based approach may also be useful for offline optimization applications, where the iterative optimization is done offline once and the result is applied in an open-loop control.

Lee *et al.*[22] took a slightly different approach. Instead of searching for the optimal state over a finite time period, which requires solving the Navier–Stokes and their adjoint equations iteratively, they looked for a *suboptimal* state, in which a control objective is minimized in the limit of the time horizon approaching zero. This adjoint-based *suboptimal control* does not require solving the governing equations iteratively. Furthermore, they showed that a wise choice of the control objective, coupled with a particular adjoint formulation (which involved taking an adjoint of only the *linear* part of the discretized Navier–Stokes equations), could lead to a more simple and practical control law. In this approach, the desired control input was expressed in terms of adjoint flow quantities at the wall, which could be evaluated without solving the adjoint equations explicitly. Minimization of a cost functional involving $\partial w/\partial y$ led to (see Lee *et al.*[22] for the detailed procedure)

$$v_w \sim \left\langle \frac{\partial}{\partial z}\frac{\partial w}{\partial y}\bigg|_w \right\rangle, \tag{4}$$

where $\langle\,\rangle$ represents a local spatial average. Note that this expression is very similar to Eq. (2), which was obtained by the adaptive neural network. The only difference in the two expressions is how high wavenumber components are reduced when the spatial average is performed; see Lee *et al.*[22] for details. Application of Eq. (4) to the turbulent channel resulted in almost identical results to those discussed in Sec. IV B, in that the computed flow field contained fewer strong near-wall streamwise vortices and skin-friction drag was reduced.

Although the two control schemes discussed in Secs. IV B and IV C were derived from totally different approaches, they yielded very similar feedback control laws. It is worth mentioning here that the adaptive nonlinear network could be approximated well by a linear network, and that the final form of the adjoint-based suboptimal control was derived without including the nonlinear part of the discretized Navier–Stokes equations when the adjoint operation was performed. It appears that whatever physics that are relevant to skin-friction drag reduction in turbulent boundary layers can be adequately approximated by a linear model.

D. Systems control theoretic approaches

Many advances have been made in linear optimal control theory over the past several decades. Unfortunately, applications of this modern control theory to flow-control problems, turbulence control in particular, have been rare. It is in large part due to the common belief that turbulent flows are nonlinear, and hence, there is very little chance that linear control theory is applicable to turbulence control. The other deterring factor might have been the fact that turbulent flows have a large number of degrees of freedom, and require analysis of a very high-dimensional system. It shall be shown here that both concerns can be overcome for control of the skin-friction drag in turbulent boundary layers.

Since the pioneering work by Joshi *et al.*,[25] in which they demonstrated that transition to turbulence (including transition due to finite-amplitude, hence nonlinear, disturbances) can be suppressed by a linear integral feedback controller, there has been a flurry of activity reporting successful applications of linear optimal control to turbulent and transitional flows.[26–31] We briefly review some fundamentals of linear optimal control theory here before we proceed to present our results. The reader is also referred to a recent paper by Bewley,[23] for an excellent introduction to linear optimal control theory as applied to fluid mechanics problems.

1. Linear optimal control and state-space representation

Linear optimal control theory starts with a state-space representation of the dynamical system to be controlled. A state-space representation of a dynamical system can be written as

$$\frac{\mathrm{d}\mathbf{x}}{\mathrm{d}t} = A\mathbf{x} + B\mathbf{u}, \tag{5}$$

where $\mathbf{x}$ represents the state vector of the system and $\mathbf{u}$ denotes the control input. The system matrix A contains the system dynamics, and B denotes an input matrix, which depends on the particular type of actuation. In linear quadratic regulator (LQR) synthesis, a cost function to be minimized is written in the following quadratic form:

$$J = \lim_{T\to\infty}\frac{1}{T}\int_0^T (\gamma \mathbf{x}^* Q\mathbf{x} + \mathbf{u}^* R\mathbf{u})\,\mathrm{d}t, \tag{6}$$

where the superscript * denotes conjugate transpose and γ is a control parameter. The matrices Q and R, respectively, represent a particular form of the control objective and how the cost of control should be accounted for. A large weighting on the cost of control (small γ) signifies a high cost of control, and vice versa. The optimal control input $\mathbf{u}$ minimizing the cost function is found in the following form:

$$\mathbf{u} = -K\mathbf{x}, \tag{7}$$

where K is the control gain matrix, which is to be determined. The optimal K minimizes the cost function, and is obtained by solving an algebraic Riccati equation involving matrices A,B,Q,R and the control parameter γ:

$$AP+PA+\gamma Q-PBR^{-1}B^{*}P=0, \tag{8}$$

from which $K=R^{-1}B^{*}P$ is determined.

Note that in the LQR synthesis, the optimal control input requires complete information of the state vector. In most practical situations, complete system information, $\mathbf{x}$, is not known, and it must be estimated based on limited measurements. This leads to linear quadratic Gaussian (LQG) synthesis, and the following dynamical system representation:

$$\frac{d\mathbf{x}}{dt}=A\mathbf{x}+B\mathbf{u}+\Gamma\mathbf{w}, \tag{9}$$

$$\mathbf{z}=C\mathbf{x}+D\mathbf{u}+\mathbf{v}, \tag{10}$$

$$\frac{d\hat{\mathbf{x}}}{dt}=A\hat{\mathbf{x}}+B\mathbf{u}+L(\mathbf{z}-\hat{\mathbf{z}}), \tag{11}$$

$$\mathbf{u}=-K\hat{\mathbf{x}}, \tag{12}$$

where $\hat{\mathbf{x}}$ denotes an estimated state vector, $\mathbf{w}$ and $\mathbf{v}$, respectively, represent system and measurement noise, which in LQG synthesis are assumed to be white Gaussian processes, $\mathbf{z}=C\mathbf{x}+D\mathbf{u}+\mathbf{v}$ denotes the actual observation, and $\hat{\mathbf{z}}=C\hat{\mathbf{x}}+D\mathbf{u}$ is the observation based on the estimated state. Matrices C,D,Γ, respectively, represent the measurement, feedthrough, and input matrices. The Kalman gain matrix L, which is designed to minimize the error associated with the estimated state, is determined in the same manner as the control gain matrix K, by solving an algebraic Riccati equation involving matrices A,C,Γ. The ratio of the power spectral densities of the noise mentioned above enters as a design parameter. In control terminology, Eq. (11) is referred to as a ''system estimator'' and Eq. (12) a ''controller,'' and together they are referred to as a ''compensator.'' In general, the system dynamics may contain many unobservable and/or uncontrollable modes, and they are neither desirable nor necessary to include in the estimator. A reduced-order model for the estimator is therefore used. This model reduction step is especially critical for turbulence control, since the original system is a very high-dimensional system, many modes of which are unobservable and uncontrollable as we normally limit our sensing and actuation to the wall. In the study to be described in Sec. IV D 5, we used a balanced-realization model-reduction method, in which the original high dimensional system is reduced by considering controllability and observability. The reader is referred to Lee *et al.*[30] for the model-reduction techniques used in the present study.

2. State-space representation of the Navier–Stokes equations

Representing the wall-normal velocity, v, and the wall-normal vorticity, ω_y, in terms of Fourier modes in the streamwise (x) and the spanwise (z) directions, the linearized Navier–Stokes (N–S) equations can be written in an operator form

$$\frac{d}{dt}\begin{bmatrix}\hat{v}\\ \hat{\omega}_y\end{bmatrix}=[A]\begin{bmatrix}\hat{v}\\ \hat{\omega}_y\end{bmatrix}, \tag{13}$$

where

$$[A]=\begin{bmatrix}L_{os} & 0\\ L_c & L_{sq}\end{bmatrix}, \tag{14}$$

and the $\hat{(\ )}$ denotes a Fourier-transformed quantity. Here L_{os}, L_{sq} and L_c represent the Orr–Sommerfeld, Squire, and the coupling operators, respectively, which are defined as

$$L_{os}=\Delta^{-1}\left(-ik_xU\Delta+ik_x\frac{d^2U}{dy^2}+\frac{1}{\mathrm{Re}}\Delta^2\right), \tag{15}$$

$$L_{sq}=-ik_xU+\frac{1}{\mathrm{Re}}\Delta, \tag{16}$$

$$L_c=-ik_z\frac{dU}{dy}, \tag{17}$$

where k_x and k_z are the streamwise and spanwise wavenumbers, respectively, $k^2=k_x^2+k_z^2$, $\Delta=\partial^2/\partial y^2-k^2$, and U is the mean velocity about which the Navier–Stokes equations are linearized.

Equation (13) is then already in the state-space representation form

$$\frac{d\mathbf{x}}{dt}=A\mathbf{x}, \tag{18}$$

where the state vector $\mathbf{x}$ consists of the wall-normal velocity and wall-normal vorticity expressed in terms of their expansion coefficients. Any polynomial expansion or collocation representation of the state vector can be used for this purpose. Having written the Navier–Stokes equations in this form, we are now in a position to design an optimal controller for this linear system.

3. Application to a linear system

Before designing and applying a linear controller to the nonlinear problem of interest, the turbulent channel, we first considered the following linear problem.

The transient growth due to non-normality of the operator associated with linearized Navier–Stokes equations has received much attention during the past several years.[32–37] It has been shown that certain disturbances can grow to $\mathcal{O}(\mathrm{Re}^2)$ in time proportional to $\mathcal{O}(\mathrm{Re})$.[35,37] It has been suggested that this transient growth, which is due to a linear mechanism, can lead to a transition to turbulence at a Reynolds number smaller than the critical Reynolds number, below which classical linear stability theory, based on modal analysis, predicts that all small disturbances decay asymptotically. Some investigators have proposed that this linear process is responsible for subcritical transition in some wall-bounded shear flows, such as plane Poiseuille flow and Couette flow. Some investigators further postulated that the same linear process is also responsible for the wall-layer streaky structures observed in turbulent boundary layers.[32,33]

Since this transient growth is due to a linear mechanism, it should be affected by a properly designed linear optimal

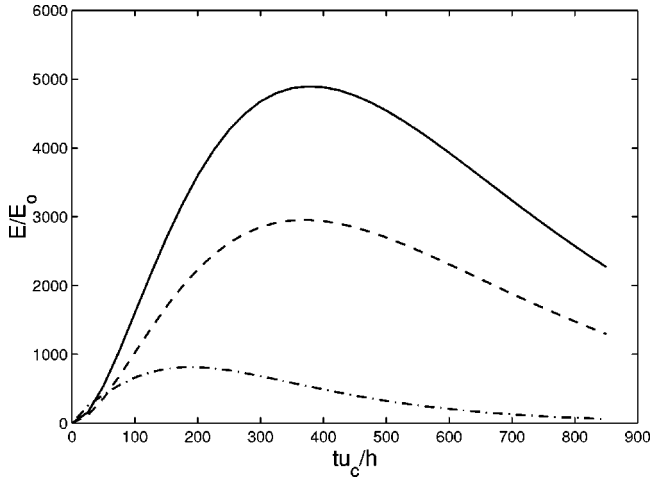

FIG. 7. Time evolution of an ''optimal'' disturbance with and without control: ——, uncontrolled; — — —, opposition control; —·—, an LQR controller.

controller, based on the linear system described in Sec. IV D 2. The so-called ''optimal'' disturbance[38] was constructed in a manner similar to that described by Butler and Farrell[32] for $Re_c=5000$, where Re_c denotes the Reynolds number based on the centerline velocity and channel half-width. Note that this is a subcritical Reynolds number with no unstable eigenmodes, but this ''optimal'' disturbance consists of a special combination of decaying eigenmodes. Due to the non-normality of the linearized Navier–Stokes operator, some of these eigenmodes are almost parallel to each other, and the energy associated with this ''optimal'' disturbance can grow initially before it ultimately decays.

An LQR controller, which minimizes the total disturbance energy, was constructed and applied to the linear system with the ''optimal'' disturbance as the initial condition. Figure 7 shows the effect of the LQR controller. Also shown in the figure is a result obtained with opposition control. It should be noted that the LQR controller utilizes complete internal state information, whereas the opposition control uses the information at a particular wall-normal location only. This explains why the LQR controller performed better than the opposition control.

4. LQR control of turbulent channel

It was not too surprising to see that a linear optimal controller worked well when applied to a linear problem. A more challenging question is whether a controller based on the linearized system would work at all in turbulent channel flow, which is obviously a nonlinear system. There are several reasons we expected a positive result in spite of the fact that turbulent channel flow is certainly beyond the scope of linear controllers. First, we saw in Secs. IV B and IV C that the wall-layer dynamics responsible for high skin-friction drag in turbulent boundary layers can be approximated well by a linear model. Second, both the transient growth mechanism in transitional boundary layers and the self-sustaining mechanism of near-wall turbulence structures in turbulent boundary layers are at least in part due to the linear mechanism described in Sec. IV D 3. Consequently, we should be able to model this linear mechanism in terms of the linear

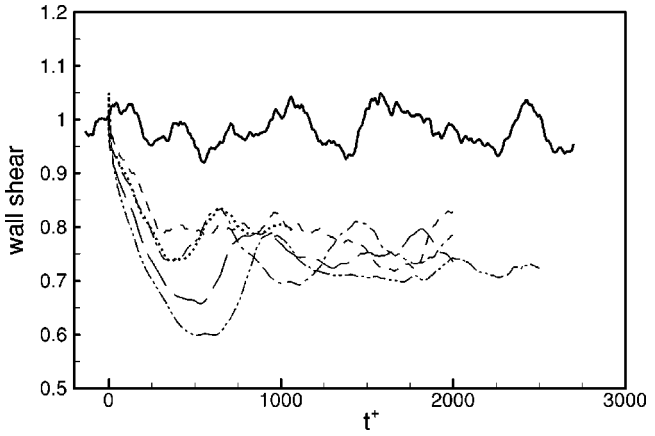

FIG. 8. Time evolution of mean wall-shear stress (normalized by its value when control started) in turbulent channel: ——, uncontrolled; others, various LQR controllers.

state-space representation, and a controller based on this linear model should be able to affect the linear mechanism.

Several LQR controllers were constructed, to minimize (1) wall-shear stress fluctuations, (2) turbulent kinetic energy, and (3) the linear coupling term (see Sec. IV E below). Results are shown in Figs. 8–10. A common feature for all of these drag-reduced flow fields is weakened streamwise vortices (Fig. 9), resulting in reduced high skin-friction extrema at the wall (Fig. 10). In some cases, especially for case (1), the controller met its design objective (i.e., it reduced fluctuating wall-shear stresses) quite dramatically, but it did not lead to similarly dramatic mean drag reduction. A further examination of the computed flow field revealed that, in contrast to opposition control, the control effect is confined to the near-wall.[39] Apparently, we need a cost function, whose minimization affects turbulence structures away from the wall. Nevertheless, all of these *linear* controllers worked remarkably well in the nonlinear flow.

The success of these linear controllers confirms, once again, the notion that a linear mechanism plays an important role in turbulent boundary layers. In a true linear system, the base (i.e., mean) flow about which the system is linearized does not evolve in time, and the system matrix A is independent of time. In a nonlinear system, however, as the state vector evolves in time, it affects the mean flow and thus A is not constant in time. One way to account for this nonlinearity is to recompute the system matrix A as the mean flow evolves. A new gain matrix K is obtained as the mean flow evolves. This can be viewed as a type of *gain scheduling*.[23] An example of LQR control with gain scheduling is shown in Fig. 11, which yields complete laminarization at $Re_\tau=100$. However, we have observed that this result was very sensitive to the manner by which the gain scheduling was implemented.[39] But this sensitivity notwithstanding, this result illustrates that a further fine tuning of linear controllers can lead to substantial improvements for nonlinear flows.

5. LQG control of turbulent channel

As mentioned in Sec. IV D 1, in most practical applications, complete state information is not available and must be estimated from limited measurements. Furthermore, the esti-

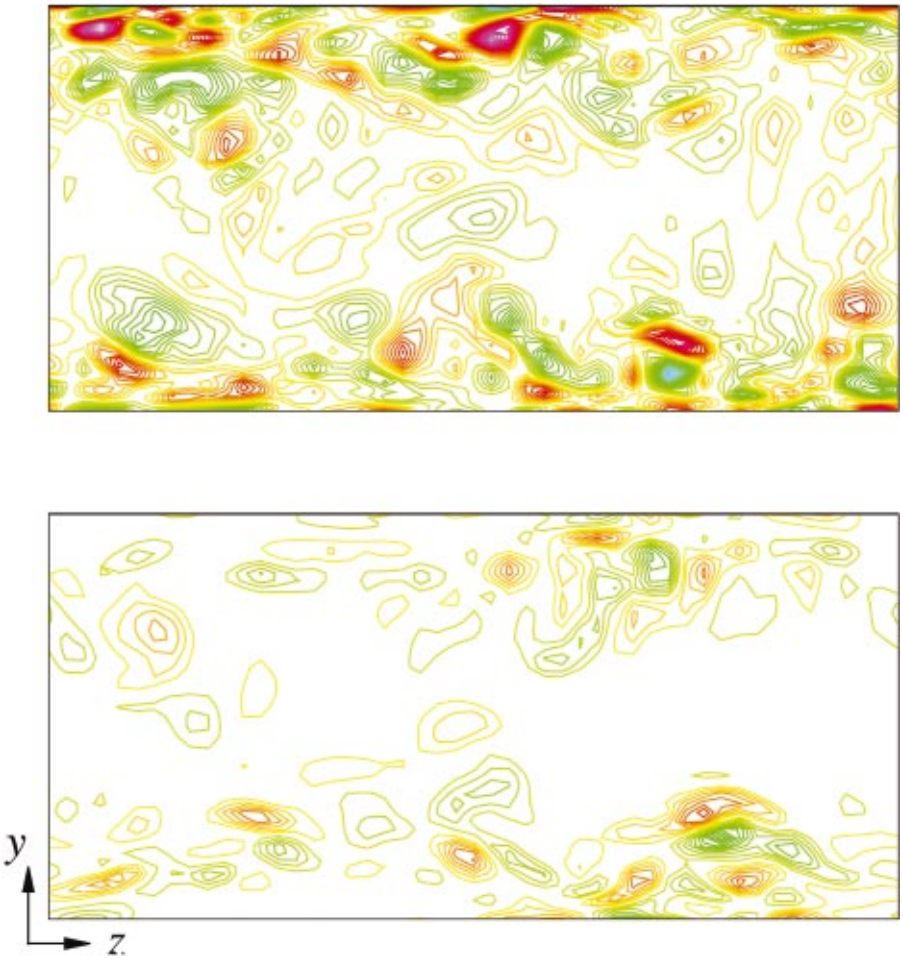

FIG. 9. (Color) Contours of streamwise vorticity in (y,z)-plane in regular channel (top) and in channel with an LQR-controller, which minimizes wall-shear stress fluctuations (bottom).

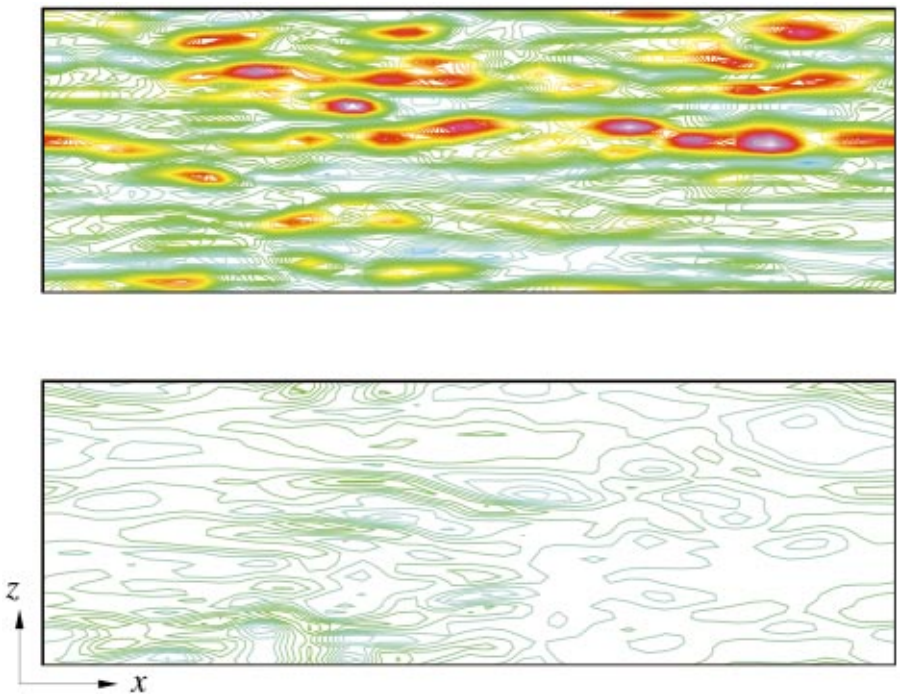

FIG. 10. (Color) Contours of wall-shear stress in (x,z)-plane in regular channel (top) and in channel with an LQR-controller, which minimizes wall-shear stress fluctuations (bottom).

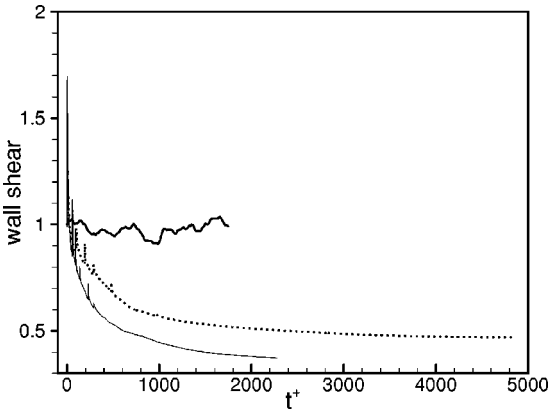

FIG. 11. Time evolution of mean wall-shear stress (normalized by its value when control started) in channel with an LQR controller, which accounts for the change of the mean flow: ——, uncontrolled; others, with a gain-scheduled LQR controller. Both gain-scheduled LQR controllers led to complete laminarization.

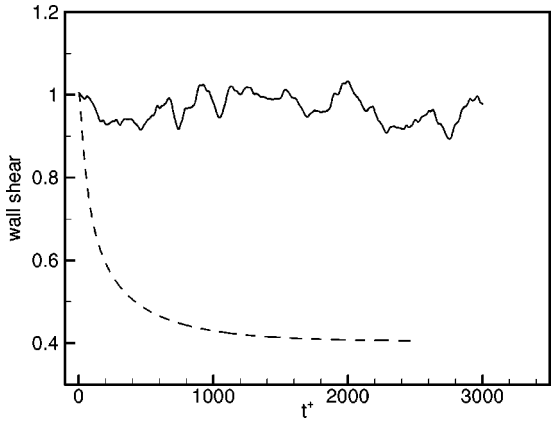

FIG. 12. Time evolution of mean wall-shear stress (normalized by its value when control started) with and without the linear coupling term: ——, regular channel; ----, channel without the coupling term.

mation must be carried out based on a reduced-order model for various reasons. Lee *et al.*[30] constructed a two-dimensional reduced-order model of the linearized Navier–Stokes system, based on controllability and observability considerations. The size of the reduced-order estimator (i.e., the number of independent modes or the length of the state vector representing the reduced-order estimator) was less than 2.5% of the original system. This two-dimensional reduced-order compensator (i.e., estimator plus controller) was applied to the turbulent channel, but Lee *et al.*[30] observed that a fully three-dimensional controller was needed; otherwise, the resulting flow patterns show substantial spanwise variations of wall-shear stress fluctuations, and they had to employ an additional *ad hoc* controller to remove the remaining spanwise variations. Lim *et al.*[39] applied an improved three-dimensional version of this LQG controller to the turbulent channel, and obtained about 20% drag reduction. The flow patterns show the same trend as those observed in the turbulent channel with LQR controllers, but the effect is confined to the near-wall region.

The performance of LQG-controllers largely depends on the performance of the estimator. We examined how well the estimator tracks the actual measurement [i.e., how small $\mathbf{z}-\hat{\mathbf{z}}$ in Eq. (11) is].[39,40] Our estimator produced excellent tracking, but the estimated internal state ranged from good (near the wall) to poor (away from the wall). Development of an improved reduced-order estimator is key to successful applications of LQG controllers, and we are currently working toward achieving this goal.

E. Reduction of non-normality in turbulent channel

The success of linear optimal controllers in the turbulent channel was somewhat unexpected, although we have shown some evidence that a linear mechanism plays an important role in turbulent boundary layers. In order to further address this question, we turn to a numerical experiment performed by Kim and Lim.[36]

They recognized that the primary reason for non-normality of the linearized Navier–Stokes system is due to L_c in Eq. (14). Although L_{os} itself is not self-adjoint (non-normal), it is L_c (referred to as the coupling term because v and ω_y are coupled through this term) that makes the operator A non-normal. Since eigenmodes of a non-normal operator are not orthogonal to each other, they allow transient growth of energy even if the individual modes are stable and decay asymptotically. Some investigators[33] suggest that this non-normal transient growth is responsible for near-wall turbulence structures in turbulent boundary layers. Kim and Lim[36] investigated the role of the coupling term in a fully nonlinear turbulent flow, by considering the following modified nonlinear system:

$$\frac{\mathrm{d}}{\mathrm{d}t}\begin{bmatrix}\hat{v}\\ \hat{\omega}_y\end{bmatrix}=\begin{bmatrix}L_{os} & 0\\ 0 & L_{sq}\end{bmatrix}\begin{bmatrix}\hat{v}\\ \hat{\omega}_y\end{bmatrix}+\begin{bmatrix}\mathcal{N}_v\\ \mathcal{N}_{\omega_y}\end{bmatrix}. \tag{19}$$

This modified system can be viewed as representing a virtual turbulent flow with no coupling term, or a turbulent flow with control by which the coupling term is suppressed (see below).

Starting from an initial field obtained from a regular turbulent channel simulation, the above modified nonlinear system was integrated in time and was compared with a nonlinear simulation with the coupling term. It was found that without the coupling term the near-wall structures first disappeared and the flow became laminar (Figs. 12 and 13). This demonstrates that the linear coupling term plays an essential role in maintaining turbulence in nonlinear flows.

Motivated by the above results, an LQR controller designed to minimize the coupling term was constructed and applied to the channel. Note that this controller can reduce the coupling term but not completely suppress it in contrast to the virtual flow above. The coupling term in the LQR-controlled flow was substantially reduced, and the strength of near-wall turbulence substantially weakened, resulting in about a 20% drag reduction.[39] An LQG controller designed to minimize the coupling term is currently under construction.

F. Beyond turbulent channel flows

The successful applications of linear controllers in the turbulent channel led us to consider more complex flows. Control of separated flow over an airfoil at a large angle of

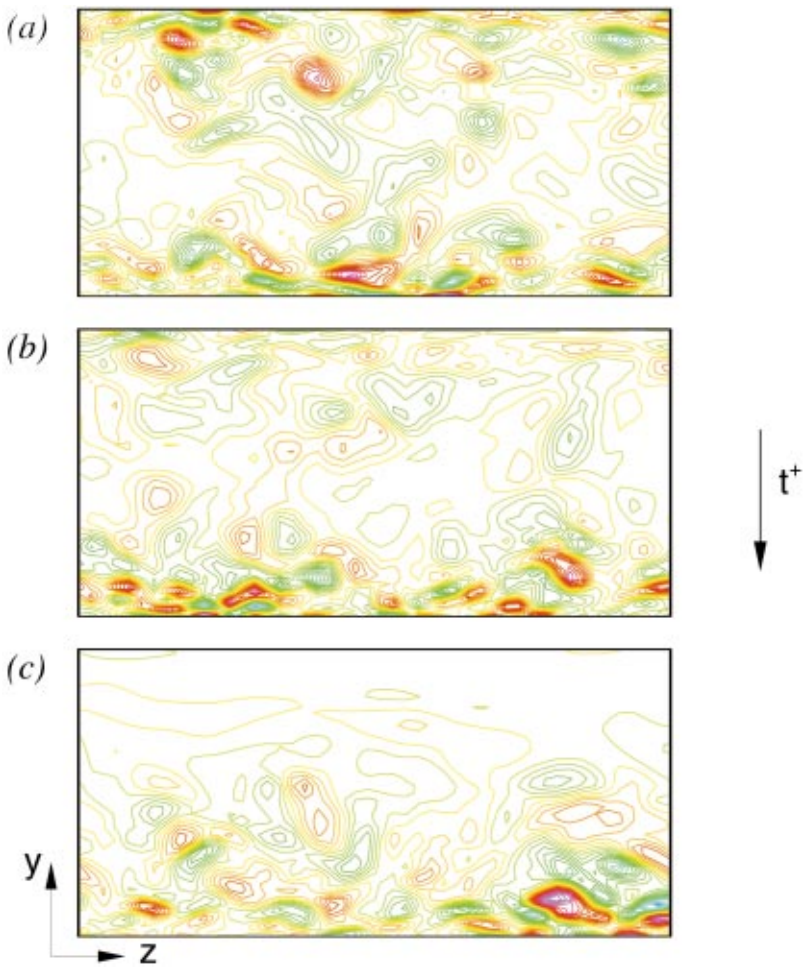

FIG. 13. (Color) Contours of streamwise vorticity in $(y-z)$-plane: (a) $t^+=0$; (b) $t^+=20$; (c) $t^+=200$. Note that $L_c=0$ only in the upper-half of the channel.

attack has been studied by many investigators owing to its technological importance. When the angle of attack is increased beyond the stall angle, the flow becomes fully separated, resulting in significant loss of lift. In many previous studies, periodic blowing and suction at a certain frequency, determined by trial and error, has been used to prevent or minimize stall at high angles of attack.

We plan to develop a control algorithm for the above-mentioned separated flow using the linear control theory discussed in Sec. IV D. Unlike the turbulent channel or turbulent boundary layer, however, turbulent flow over an airfoil cannot be easily converted into a state-space representation, since the required system information (matrices A, B, C and D) is difficult to obtain. In a situation like this, system identification approaches can be used to model the input/output relationship of the system. Once an approximate model for this complex flow is identified, the same procedure used in channel flow control can be used to design optimal controllers. The underlying assumption here, of course, is that some key dynamics of the separated flow can be captured by a linear model. Whether this assumption is valid, and how successful the approximate model obtained via system identification techniques turns out to be, remains to be seen.

V. ISSUES, LIMITATIONS AND CONCLUSION

I have presented a few successful applications of controllers that are fundamentally different from many existing ones in that they were derived from linear control theory, which has not been widely embraced by the fluid mechanics community. These successes are quite promising, as they suggest a new approach for turbulence control, a topic which has been viewed by many as beyond the scope of linear control theory. It turns out that in wall-bounded shear flows a linear mechanism plays an important role in near-wall turbulence dynamics, especially from the perspective of skin-friction drag. This linear mechanism, which exists in the presence of other fundamental nonlinear processes, can be captured by a linear model, and much can be accomplished by utilizing linear control theory. There is some evidence that further fine tuning may lead to even better performance than that shown here. However, there are many outstanding issues that must be resolved before this approach can be fully implemented. Some of these issues are listed below. They are neither in any particular order, nor exhaustive; they simply reflect issues that have come to light during the course of this work.

(1) Model reduction. An improved model reduction technique is key to successful applications of linear control theory to flow control in general, and turbulence control in particular. Currently we use a balanced-realization model-reduction approach, in which the original high-dimensional system is reduced by considering controllability and observability. A reduced-order model should retain the essential features of the original dynamical

system. Most existing model-reduction techniques, including ours, aim at reproducing the input–output relationship of the original system, thus accounting for controllability and observability, but they do not account for the control objective. This is certainly not desirable, as it may leave out some important system dynamics, which are relatively less observable or controllable, but nevertheless may contribute significantly to the control objective. Ideally, all three aspects (control objective, controllability and observability) should receive proper weight during the model reduction stage. In this regard, it is worth mentioning that a model reduction purely based on POD (proper orthogonal decomposition) modes may not be appropriate since it gives no consideration to controllability and observability, and perhaps (at least not directly) to the control objective, either.

(2) Control objective (or cost function). For the purpose of drag reduction, we have considered several control functions to be minimized (note that the drag itself, which is a mean quantity, cannot be incorporated directly into the cost function), but they are not necessarily the most appropriate ones. In fact, in some examples given here, controllers performed extremely well from the point of minimizing the given cost function—in other words, the controllers met the design objective—but unfortunately they did not lead to correspondingly significant reduction in the mean drag. Whether this implies an inherent limitation of linear controllers for nonlinear flows or simply calls for different cost functions has not yet been determined.

(3) Localized control. All examples shown in this paper used controllers designed and applied in wavenumber space. Measurements from distributed sensors are collected and converted into Fourier space, where control input (actuation) is determined and applied (actuation itself can be applied in physical space by converting the control input back to physical space, but that is beside the point). The primary reason behind this approach was that the linearized Navier–Stokes system completely decouples for each wavenumber, thus converting a large linear system into a small linear system for each wavenumber. However, this procedure, which is sometimes referred to as a centralized approach[23] (since it requires central processing of data), requires global sensor information for each actuator. A more desirable approach would be one in which the control input for each actuator is determined solely by information obtained by neighboring sensors, as in

$$\mathbf{u}(x,z,t)=\int G(x-\xi,z-\eta)\mathbf{z}(\xi,\eta,t)\mathrm{d}\xi\mathrm{d}\eta, \tag{20}$$

where G denotes a control kernel in physical space. A key consideration of this approach (referred to as localized or decentralized control) is how well the control kernel can be localized in physical space, which allows determination of the control input, $\mathbf{u}(x,z,t)$, based on local $\mathbf{z}(x,z,t)$. There is some evidence that this is indeed possible,[23,39] but it requires further investigation.

(4) Actuator. In our numerical experiments, we have used the wall-shear stresses as measurements (sensing) and surface blowing and suction as control input (actuation). Shear-stress sensors are currently available and pose no practical problems, but actuators that can deliver the same type of blowing and suction at the wall are not yet available.[41] Furthermore, in our numerical experiments, we have not accounted for any time delay between sensing and actuation, whereas in practice there will be a finite delay due to both actuator response time and data processing time.

(5) Numerical issues. Although this is not a control issue, it is worth mentioning here that the system matrix we have to deal with is extremely poorly conditioned (i.e., it has a high condition number) and all computations (e.g., transforming into a Jordan form for model reduction, solving the Riccati equations for the control and estimator gain matrices, etc.) involving the system matrix must be done with care. The effect of under-resolved modes (due to a finite-dimension representation of the infinite-dimension system) and the effect of spurious modes (due to a particular state-space representation) are other examples that require special attention. Some of these modes can be very controllable and/or observable, and therefore can adversely affect the controller design and its performance.

(6) Reynolds number. All successful examples thus far, including those conducted by other investigators and not presented here, have been at very low Reynolds numbers. Some investigators believe that there are fundamental changes in the turbulent transport processes in turbulent boundary layers at high Reynolds numbers.[42] Therefore, all current approaches that control near-wall turbulence structures, which according to these investigators are only relevant to low Reynolds number flows, may not be applicable to turbulent boundary layers at high Reynolds numbers. This remains to be seen. It is worth noting, however, that the riblet surface, which also affects near-wall turbulence structures, has been proven to reduce skin-friction drag during a flight test of a commercial aircraft—an example illustrating that what worked at low Reynolds numbers (both in numerical and laboratory experiments) also worked at a high Reynolds number.

(7) Beyond simple flows. It will be extremely interesting to see how far we can push the current approach toward more realistic and complex flows for which we do not have complete system information. The system identification approach is one way to tackle this problem, but it remains to be seen how robust this approach will be, especially for nonlinear flows.

In summary, I have shown that applications of linear control theory to a particular problem of turbulence control result in quite promising results. This is due in large part to the important role of certain linear mechanisms in wall-bounded shear flows. Exploitation of linear mechanisms in other flows may also lead to successful results. Although control theory has emerged as a viable and powerful tool for flow-control problems, there remain many outstanding is-

sues. I expect that further collaborations between control theoreticians and fluid dynamicists will lead to even greater progress in the future.

ACKNOWLEDGMENTS

I would like to thank my former and current students, postdocs and colleagues at UCLA, Professor Jason Speyer in particular, who has enlightened me about control theory. I would also like to thank my former colleagues at NASA Ames Research Center and Stanford University, Alan Wray, Bob Rogallo, Bill Reynolds and Parviz Moin in particular, from whom I have learned much about turbulence and turbulence simulations. Without their help, winning such a prestigious award would not have been possible; I have been lucky to be where I have been at the right time with the right people. I also gratefully acknowledge the sustained financial support provided by the Air Force Office of Scientific Research (program managers: Dr. James McMichael, Dr. Mark Glauser, Dr. Tom Beutner, Dr. Marc Jacobs, and Dr. Berlinda King) and by the Office of Naval Research (program manager: Dr. Pat Purtell) during the course of this work. The computer time provided by NASA Ames Research Center and NSF NPACI Centers is also gratefully acknowledged. Finally, I thank Dr. Gary Coleman for his comments on a draft of this manuscript and Junwoo Lim for providing some figures used in this paper.

[1]D. M. Bushnell, private communication, 1996. A 10% reduction in fuel cost of commercial aircraft would yield a 40% increase in the profit margin of an airplane.
[2]P. Moin and K. Mahesh, ''Direct numerical simulation: A tool in turbulence research,'' Annu. Rev. Fluid Mech. **30**, 539 (1998).
[3]T. Tsao, F. Jiang, C. Liu, R. Miller, S. Tung, J.-B. Huang, D. Babcock, C. Lee, Y.-C. Tai, C.-M. Ho, J. Kim, and R. Goodman, ''MEMS-based active drag reduction in turbulent boundary layers,'' in *Microengineering Aerospace Systems*, edited by H. Helvajian (The Aerospace Press, Los Angeles, 1999).
[4]C.-M. Ho and Y.-C. Tai, ''Micro-electro-mechanical-systems (MEMS) and fluid flows,'' Annu. Rev. Fluid Mech. **30**, 579 (1998).
[5]K. Zhou, J. C. Doyle, and K. Glover, *Robust and Optimal Control* (Prentice Hall, Englewood Cliffs, NJ, 1996).
[6]P. Moin and J. Kim, ''Numerical investigation of turbulent channel flow,'' J. Fluid Mech. **118**, 341 (1982).
[7]The original plan was for the ILLIAC IV to be used by scientists at the University of Illinois, but student demonstrations led to its removal out of the University. Dr. Hans Marc, then Director of NASA Ames Research Center and a theoretical physicist by training, seized the opportunity to bring the computer to Ames Research Center as he forsaw what the powerful computer could do for scientific research.
[8]I am much indebted to Alan Wray for recollecting technical details of ILLIAC IV mentioned in this paper.
[9]S. J. Kline, W. C. Reynolds, F. A. Schraub, and P. W. Runstadler, ''The structure of turbulent boundary layers,'' J. Fluid Mech. **30**, 744 (1967).
[10]H. Choi, P. Moin, and J. Kim, ''Direct numerical simulation of turbulent flow over riblets,'' J. Fluid Mech. **255**, 503 (1993).
[11]A. G. Kravchenko, H. Choi, and P. Moin, ''On the relation of near-wall streamwise vortices to wall skin friction in turbulent boundary layers,'' Phys. Fluids A **5**, 3307 (1993).
[12]J. Kim, P. Moin, and R. D. Moser, ''Turbulence statistics in fully developed channel flow at low Reynolds number,'' J. Fluid Mech. **177**, 133 (1987).
[13]J. M. Hamilton, J. Kim, and F. Waleffe, ''Regeneration mechanisms of near-wall turbulence structures,'' J. Fluid Mech. **287**, 317 (1995).
[14]F. Waleffe and J. Kim, ''How streamwise rolls and streaks self-sustain in a shear flow,'' in *Self-Sustaining Mechanisms of Wall Turbulence*, edited by R. Panton (Computational Mechanics, Southampton, 1997).
[15]J. Jiménez and A. Pinelli, ''The autonomous cycle of near-wall turbulence,'' J. Fluid Mech. **389**, 335 (1999).
[16]W. Schoppa and H. Hussain, ''Coherent structure generation in near-wall turbulence,'' J. Fluid Mech. **453**, 57 (2002).
[17]In our original paper, we used the second-order Adams–Bashforth (AB) method. Since then it has been switched to a low-storage third-order Runge–Kutta (RK) scheme. The third-order RK scheme is the preferred method, and I mention this here as I have noticed that many investigators are still using the second-order AB method in similar calculations, perhaps due to our original report.
[18]H. Choi, P. Moin, and J. Kim, ''Active turbulence control for drag reduction in wall-bounded flows,'' J. Fluid Mech. **262**, 75 (1994).
[19]E. P. Hammond, T. R. Bewley, and P. Moin, ''Observed mechanisms for turbulence attenuation and enhancement in opposition-controlled wall-bounded flows,'' Phys. Fluids **10**, 2421 (1998).
[20]C. Lee, J. Kim, D. Babcock, and R. Goodman, ''Application of neural networks to turbulence control for drag reduction,'' Phys. Fluids **9**, 1740 (1997).
[21]H. Choi, R. Teman, P. Moin, and J. Kim, ''Feedback control for unsteady flow and its application to the stochastic Burgers equation,'' J. Fluid Mech. **253**, 509 (1993).
[22]C. Lee, J. Kim, and H. Choi, ''Suboptimal control of turbulent channel flow for drag reduction,'' J. Fluid Mech. **358**, 245 (1998).
[23]T. R. Bewley, ''Flow control: New challenges for a new Renaissance,'' Prog. Aerosp. Sci. **37**, 21 (2001).
[24]T. R. Bewley, P. Moin, and R. Temam, ''DNS-based predictive control of turbulence: An optimal benchmark for feedback algorithms,'' J. Fluid Mech. **447**, 179 (2001).
[25]S. S. Joshi, J. L. Speyer, and J. Kim, ''A systems theory approach to the feedback stabilization of infinitesimal and finite-amplitude disturbances in plane Poiseuille flow,'' J. Fluid Mech. **332**, 157 (1997).
[26]S. S. Joshi, J. L. Speyer, and J. Kim, ''Finite dimensional optimal control of Poiseuille flow,'' J. Guid. Control Dyn. **22**, 340 (1999).
[27]T. R. Bewley and S. Liu, ''Optimal and robust control and estimation of linear paths to transition,'' J. Fluid Mech. **365**, 305 (1998).
[28]L. Cortelezzi, K. Lee, J. Kim, and J. L. Speyer, ''Skin-friction drag reduction via robust reduced-order linear feedback control,'' Int. J. Comput. Fluid Dyn. **11**, 79 (1998).
[29]L. Cortelezzi and J. L. Speyer, ''Robust reduced-order controller of laminar boundary layer transitions,'' Phys. Rev. E **58**, 1906 (1998).
[30]K. Lee, L. Cortelezzi, J. Kim, and J. L. Speyer, ''Application of reduced-order controller to turbulent flows for drag reduction,'' Phys. Fluids **13**, 1321 (2001).
[31]A special symposium on this topic was held during the 54th American Physical Society Division of Fluid Dynamics meeting in San Diego, CA, 16–18 November 2001. The interested reader is referred to Bull. Am. Phys. Soc. **46** (10) (November 2001).
[32]K. M. Butler and B. F. Farrell, ''Three-dimensional optimal perturbations in viscous shear flow,'' Phys. Fluids A **4**, 1637 (1992).
[33]K. M. Butler and B. F. Farrell, ''Optimal perturbations and streak spacing in wall-bounded turbulent shear flow,'' Phys. Fluids A **5**, 774 (1993).
[34]S. C. Reddy and D. S. Henningson, ''Energy growth in viscous channel flows,'' J. Fluid Mech. **252**, 209 (1993).
[35]B. F. Farrell and P. J. Ioannou, ''Stochastic forcing of the linearized Navier–Stokes equations,'' Phys. Fluids A **5**, 2600 (1993).
[36]J. Kim and J. Lim, ''A linear process in wall-bounded turbulent shear flows,'' Phys. Fluids **12**, 1885 (2000).
[37]B. Bamieh and M. Dahleh, ''Energy amplification in channel flows with stochastic excitation,'' Phys. Fluids **13**, 3258 (2001).
[38]From a control point of view, this is actually the ''worst'' disturbance; we employ this commonly-used term in quotes to avoid confusion with optimal control.
[39]J. Lim, ''Control of wall-bounded turbulent shear flows using modern control theory,'' Ph.D. dissertation, University of California, Los Angeles, 2003.
[40]J. Lim, J. Kim, S. Kang, and J. L. Speyer, ''Linear controllers for turbulent boundary layers,'' Bull. Am. Phys. Soc. **46**, 156 (2001).
[41]A synthetic jet comes close as far as the blowing is concerned. The flow pattern during the suction phase of a syntheic jet is, however, quite different from that of the surface suction used in the numerical experiment.
[42]J. C. R. Hunt, private communication, 2001.